

Efficient Fuzzy Binarization for Automatic Ganglion Cyst Extraction from Ultrasound Images

Seung-Ik Park¹, Doo Heon Song², and Kwang Baek Kim^{1*}

¹*Department of Computer Information, Silla University, Busan, Korea.*

²*Department of Computer Games, Yong-In SongDam College, Yong-in, Korea.*

In this paper, we propose an efficient image quality enhancement strategy for automatic ganglion cysts extraction from ultrasound images. With such improved intensity contrast, it becomes easier to differentiate the cyst from the surrounding mass. In order to achieve our goal, we propose a fuzzy binarization method with trapezoid type membership function that has dynamic adjustment of critical section in binarization. In experiment with real world cyst cases, the proposed method successfully extracted ganglion cysts in 42 out of 45 cases (93.3%) accurately which is far better than Average binarization method and static fuzzy binarization with triangle membership function. Fuzzy stretching component also contributes to this performance enhancement in that it gives far better result than usual normalization in intensity contrast enhancement and cyst extraction performance. With this automatic ganglion cyst detecting software, medical experts can find cyst area without operator subjectivity in order to make better diagnosis.

Keywords: ganglion cyst; fuzzy binarization; trapezoid automatic extraction; fuzzy stretching

I. INTRODUCTION

Ganglion cysts are benign soft tissue tumors that are commonly encountered in the wrist but it may occur in any joint such as shoulder and elbow. Cyst can change their size or disappear completely without reason in some cases but it may reappear at any time (Freire *et al.*, 2012). In many cases, ganglion is anechoic, posterior enhancement and has relatively well-defined margin. It is often seen as monotonic, but it may be accompanied by internal diaphragm or it may appear to be multilocular (Yoo, 2014).

On examination, wrist ganglions are usually 1–2 cm cystic structures, feeling much like a firm rubber ball that is well tethered in place by its attachment to the underlying joint capsule or tendon sheath (Gude & Morelli., 2008). In the case of intraosseous ganglion in some bones, the cortical bone may be thinned or broken due to expansion of the cystoma, and avascular necrosis may cause carpal bones),

resulting in continuous pain and development of a pathological fracture (Yamazaki *et al.*, 2007).

Although it can be easily diagnosed by clinical features or location, there may be confusion with other masses if it is accompanied by complications or when it occurs in unusual site (Kim, 2015). The ganglion adjacent to the radial artery near the radiocarpal joint may be pulsatile and that may cause a possible clinical misidentification as a pseudoaneurysm (Kwon *et al.*, 2001).

There are nonsurgical and surgical option to treat ganglion cyst. Nonsurgical treatments of ganglion including aspiration, steroid injection sclerotherapy, and hyaluronidase were generally ineffective. However, since they had lower complication rates, they can be used for symptomatic relief if the patients do not want surgery. Open surgical excision had a lower recurrence rate than conservative treatment. However, it has higher rates of complication and longer recovery period, and the rate of symptomatic relief may not be higher than other treatments

*Corresponding author's e-mail: gbkim@silla.ac.kr

(Suen *et al.*, 2013). Mean recurrence rates across all study designs were congruent with meta-analysis findings. Open surgical excision had a mean recurrence of 21%, compared with a recurrence rate of 59% for aspiration (Head *et al.*, 2015).

Ultrasonography is, in general, an effective imaging method for evaluating a palpable soft tissue abnormality with the strength of its ability to differentiate a solid mass from a cyst and for its non-invasive, inexpensive, real time responses. In treatment phase, ultrasonography also gives a guidance for aspiration and injection (Yamazaki *et al.*, 2007; Wang *et al.*, 2007). Ultrasonography can diagnose ganglion with similar accuracy to magnetic resonance imaging, and it is rather advantageous to distinguish it from a small amount of joint fluid (Kang *et al.*, 2014). However, the common complaint against using ultrasonography in medical diagnosis is its well-known operator subjectivity (Gress *et al.*, 2001). That is, the quality of the diagnosis is dependent on the qualities of equipment and skills of expertise. Thus, we need an automatic image segmentation and identification tool for anatomical landmarks that can eliminate such subjectivity in the image analysis (Enikov & Anton, 2014). Automatic segmentation in ultrasound images, though, can be difficult for numerous reasons such as insufficient contrast and resolution of image, speckle noise which is inherent property of ultrasound imaging modality, and more (Gupta *et al.*, 2014, Kim *et al.*, 2018).

In this paper, we propose a method to extract ganglion cyst area from ultrasound images automatically by fuzzy binarization. This automatic segmentation of the target organ object usually consists of two phases – intensity contrast enhancement and object formation. In intensity contrast enhancement phase, one may use standard normalization process (Gonzalez & Woods, 2002) or fuzzy stretching with relatively heavier computation (Kim, 2015). In object forming phase, one may apply pixel clustering algorithms to differentiate target object from the surroundings or just apply a series of image processing algorithms to form a cyst object after binarization process. Pixel clustering approaches (Park *et al.*, 2017; Suryadibrata & Kim, 2017; Suryadibrata *et al.*, 2017) decide the membership of a pixel to a clustered object based on fuzzy logic or neural network so that the automatic cyst detecting algorithm was not necessarily dependent from the shape assumption. Unfortunately, such efforts have pros and cons. Pixel clustering was successful in soft tissue tumor detection (Park *et al.*, 2017) but not for the ganglion cyst to

meet the practical standard. An approach with Possibilistic C-Means (PCM) looked like strong against speckle noise but had a tendency to underestimate the cyst region especially when candidate objects are overlapped (Suryadibrata & Kim, 2017). Fuzzy C-Means (FCM) based approach in forming clusters showed better result but it still suffered from object disconnection problem during learning and our retrospective analysis concluded that we need better image enhancement policy to overcome the difficulty of cyst forming during FCM (Suryadibrata *et al.*, 2017).

Thus, we focus on the intensity enhancement and binarization process in this paper. We take fuzzy stretching again but let the process be adaptive to the environment which was successful in other engineering domain (Kim & Song, 2017). Then, we apply fuzzy binarization with trapezoid membership function to differentiate the target organ from the environment. Object forming process consists of 8-directional contour tracking and object labelling instead of computationally expensive pixel clustering algorithms.

II. MATERIALS AND METHODS

The proposed method consists of fuzzy stretching, fuzzy binarization, and object forming process.

A. Fuzzy stretching

Image enhancement with fuzzy logic is known to be relatively noise tolerant (Shin & Jung, 2017). We use dynamically controlled fuzzy stretching in this paper. The image may not have enough brightness contrast between the “bright” side and the “dark” side. We stretch 0’s and 1’s as follows so that the bright contrast is effectively exaggerated to find the boundary lines as accurate as possible.

$$X_m = \sum_{i=0}^{255} X_i^* \frac{1}{M^*N} \quad (1)$$

Let X_m be the average brightness value of the image with $M \times N$ size, the distance from the brightest pixel and the darkest pixel are defined as equation (2).

$$\begin{aligned} D_{\max} &= |X_h - X_m| \\ D_{\min} &= |X_x - X_l| \end{aligned} \quad (2)$$

The brightness adjustment value is computed as shown in equation (3).

$$\begin{aligned}
 &\text{if } (X_m > 128) \text{ adjustment} = 255 - X_m \\
 &\text{else if } (X_m \leq D_{\min_{\min}}) \\
 &\text{else if } (X_m \geq D_{\max}) \text{ adjustment} = D_{\max} \\
 &\text{adjustment} = X_m
 \end{aligned} \quad (3)$$

Thus, the maximum, minimum, and the center point of the brightness which will form the fuzzy membership triangle are defined as equation (4);

$$\begin{aligned}
 I_{\max} &= X_m + \text{adjustment} \\
 I_{\min} &= X_m - \text{adjustment} \\
 I_{\text{mid}} &= \frac{I_{\max} + I_{\min}}{2}
 \end{aligned} \quad (4)$$

The membership function of each pixel in the region of interest (ROI) is given as Fig. 1.

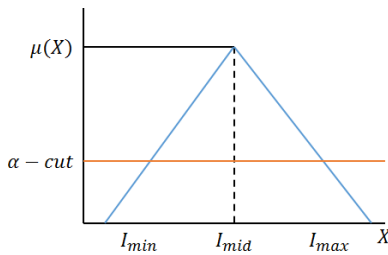


Figure 1. Membership function for stretching

where I_{\min} , I_{\max} be the minimum and maximum brightness of the given region and I_{mid} be the midpoint of the two.

The cut point (α -cut) in Figure 1 is computed as follows;

$$\begin{aligned}
 &\text{if } (I_{\min} > 0) \alpha - \text{cut} = I_{\min}/I_{\max} \\
 &\text{else } \alpha - \text{cut} = 0.5
 \end{aligned} \quad (5)$$

The degree of membership of a pixel $\mu(X)$ is defined as formula (6).

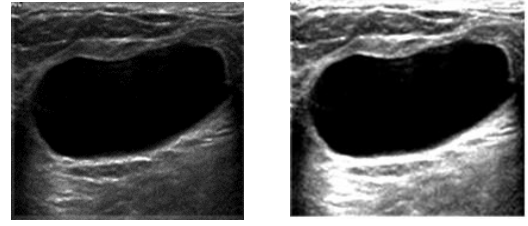
$$\begin{aligned}
 &\text{if } (X_m \leq I_{\min}) \text{ or } (X_m \geq I_{\max}) \text{ then } \mu(X) = 0 \\
 &\text{if } (X_m > I_{\text{mid}}) \text{ then } \mu(X) = \frac{I_{\max} - X_m}{I_{\max} - I_{\text{mid}}} \\
 &\text{if } (X_m < I_{\text{mid}}) \text{ then } \mu(X) = \frac{X_m - I_{\min}}{I_{\text{mid}} - I_{\min}}
 \end{aligned} \quad (6)$$

The upper limit value (β) and the lower limit value (α) are defined as the highest and lowest X_i among pixels that have higher membership degree than the cut point (α -cut).

Then the final stretched value of the pixel is computed by formula (7).

$$X_{\text{new}} = \frac{X - \alpha}{\beta - \alpha} \times 255 \quad (7)$$

The effect of fuzzy stretching is shown as Fig. 2.



(a) Input Image (b) After Fuzzy Stretching

Figure 2. The effect of fuzzy stretching

B. Fuzzy binarization

After stretching, we need to differentiate pixels of the target object from surroundings by binarization process. In this process, we need environment adaptive dynamic threshold for the robustness. Since binarization process decides if a pixel's intensity is 0 or 1, we need more flexible membership function than usual triangle shape. Trapezoidal membership function works practically well in engineering problems (Kim *et al.*, 2014, Woo & Kim, 2016) and there exists a theoretical ground for its appropriateness (Barua *et al.*, 2014). Also, we apply dynamic cut-point again to adapt low intensity contrast images. Thus, the membership function for binarization looks like Figure 3.

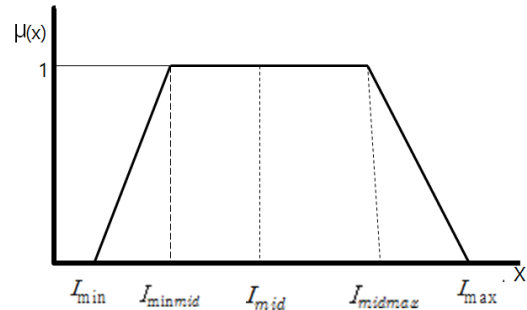


Figure 3. Membership function for binarization

Let V_{\max} , V_{\min} be the maximum and minimum intensity value of the mage. Then, the intensity rate X_n is defined as equation (8).

$$X_n = V_{\max}/V_{\min} \quad (8)$$

Then a similar process to define the intensity adjustment rate as given in equation (2) and (3) is given as following equation (9).

$$\begin{aligned}
 D_{D_{max}} &= |X_{max} - X_n| \\
 D_{D_{min}} &= |X_n - X_{min}| \\
 \text{if } (X_n > 128) &\text{ then } \theta = 255 - X_n \\
 \text{else if } (X_n \leq D_{D_{min}}) &\text{ then } \theta = D_{D_{min}} \\
 \text{else if } (D_{D_{max}} \geq X_n) &\text{ then } \theta = D_{D_{max}} \\
 \text{else } \theta &= X_n
 \end{aligned} \quad (9)$$

Now, the interval variables of trapezoidal membership function shown in Fig. 3 are defined as equation (10).

$$\begin{aligned}
 I_{max} &= X_m + \theta \\
 I_{min} &= X_m + \theta \\
 I_{mid} &= \frac{I_{max} + I_{min}}{2} \\
 I_{min\ mid} &= |X_m - X_n| \\
 I_{mid\ max} &= |X_m + X_n|
 \end{aligned} \quad (10)$$

And the dynamic threshold controller variable is defined as following equation (11).

$$\begin{aligned}
 \delta &= \{I_{mid} + (I_{min\ mid} + I_{mid\ max})/2\}/255 \\
 \alpha - cut &= (\delta + 0.5) \wedge 1
 \end{aligned} \quad (11)$$

where \wedge is the fuzzy minimum operator.

Thus, the intensity of a pixel becomes 0 if the membership degree of Fig. 3 is larger than the cut-point. The effect of the fuzzy binarization is as shown in Fig. 4.

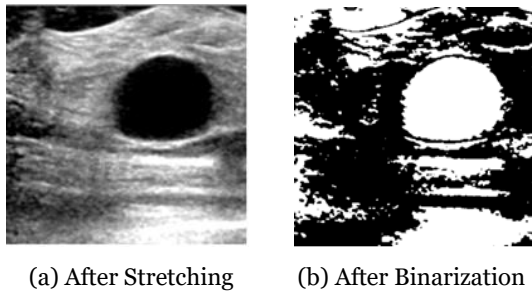


Figure 4. The effect of fuzzy binarization

C. Cyst object formation

After binarization, we apply 8-directional contour tracking algorithm (Kim *et al.*, 2006) to remove noises and other outside area of the ganglion. Using masks, the tracking algorithm scans the image from up to bottom and left to right. When a black pixel (intensity 255) is found after applying the tracking mask in the current pixel, the next tracking pixel is decided from the right side of the current pixel as rotating clockwise. When the tracking is finished, remove object whose intensity is 0 or too small in size (less than 1/4 of the ROI in this paper) as noise. Then the target

object is found as shown in Fig. 5 which is the candidate of ganglion cyst.

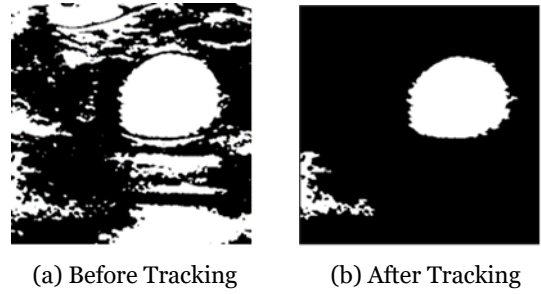


Figure 5. The effect of 8-directional contour tracking

Then, we apply erosion and dilation operators to refine the boundaries of the candidate objects. The largest oval-like object in the ROI is the target ganglion cyst as shown in Fig. 6 after labelling procedure.

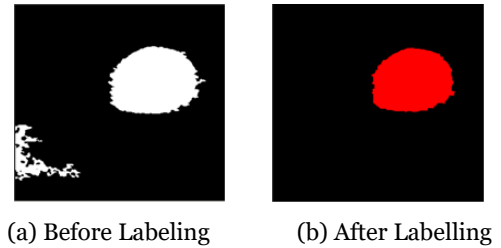


Figure 6. Cyst extraction example

III. RESULT AND DISCUSSION

The experiment is implemented using Visual Studio 2013 C# with Intel® Core™ i5-5200 CPU @ 2.80GHz and 3GB RAM with 45 wrist ultrasonography images containing ganglion cysts from Gupo Hospital, Busan, Korea. Two radiologists of the hospital participated in this experiment and images are obtained by Philips iU22 (2016 edition) using 7-17 MHz high frequency linear probe. Participated radiologists decide if the ganglion cyst of the image is successfully extracted.

The performance of the proposed method is compared with the baseline competitor that uses average binarization with Ends-in stretching (usual normalization). The result is summarized in Table 1.

Table 1. Cyst Extraction Performance Evaluation

| Method | Success | Failure | Success rate |
|----------|---------|---------|--------------|
| Proposed | 42 | 3 | 93.3% |
| Baseline | 34 | 11 | 75.6% |

The proposed method uses two components – fuzzy stretching and fuzzy binarization. First, we analyze the binarization effect as following.

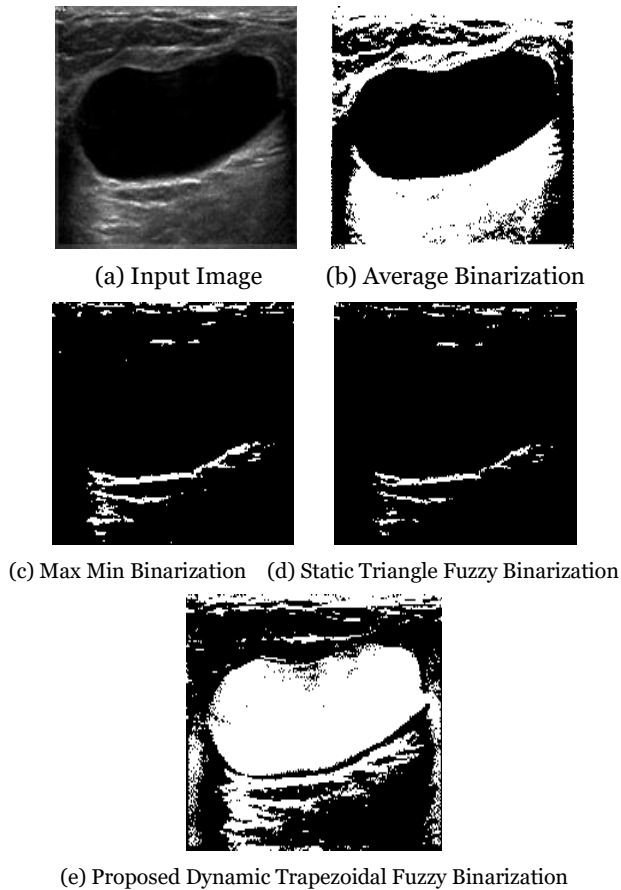


Figure 7. Example of Various Types of Binarization Results

The input image of Fig. 7(a) is a typical example of low intensity contrasted large cyst. The intensity distribution is relatively simpler than others. Average binarization method (Fig. 7(b)) can form a cyst but the boundary lines are not smooth and partially overlapped with the background on both sides of the cyst object. The threshold value in this particular example was 43.

When we apply Max-Min binarization (Fig. 7(c)) in order to overcome such boundary information loss problem, the threshold was computed as 127 thus too many pixels are converted to black pixels and the cyst object became not recognizable.

The static α -cut (0.5) with usual triangle fuzzy membership function does not work either (Fig. 7 (d)). The membership function interval was too narrow ($[0, 149]$ in this example) to protect boundary lines and cyst object pixels.

The proposed method, however, was successful in adapting to the environment and showed the least information loss as shown in Fig. 7 (e) and the membership function interval was

$[0, 193]$ and the cut point was 0.65 thus it can cover the most meaningful area of cyst object.

Although it is not theoretically sound why triangle membership function fails but the trapezoidal function works in this case, our speculation is that the intensity distribution is too simple in this image. With adaptive cut-point, the trapezoidal fuzzy membership function is more scale-invariant and shift invariant (Barua *et al.*, 2014) thus it has domain specific advantages over triangle membership function.

Table 2. Effect of Fuzzy Stretching

| Method | Success | Partially Success | Failure |
|---------------|---------|-------------------|---------|
| Proposed | 42 | 1 | 2 |
| Normalization | 37 | 2 | 6 |

The fuzzy stretching component of the proposed method also contributes to the successful extractions. If we change our fuzzy stretching with Ends-in stretching (usual normalization), the successful cyst extraction rate decreases to 82.2% (37 out of 45 cases) as shown in Table 2.

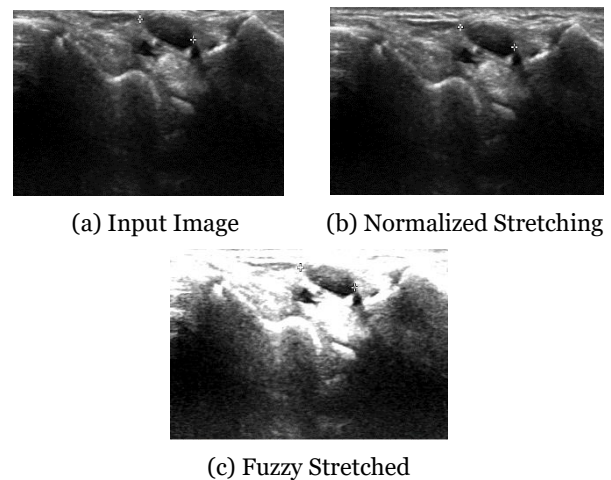


Figure 8. Stretching Comparisons

As shown in Fig. 8, when we use normalization instead of proposed fuzzy stretching, the intensity contrast was not sufficiently enhanced and as a result, the case of Fig. 8(b) was later classified into partially successful extractions in Table 2 while the proposed method was fully successful in extraction.

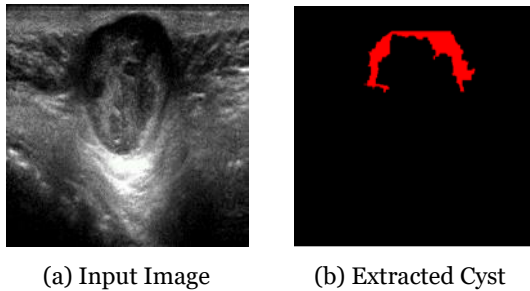


Figure 9. Failed Extraction Case

Unfortunately, there were a few failed extraction cases as shown in Fig. 9. In most cases, ganglion cysts have an oval-like shape. However, in this case, the lower part of the cyst is unusually bright thus indistinguishable from its surroundings. Such case can happen if the ultrasonography shows solid mass characteristics. In such cases, there may be hemorrhage inside the ganglion, or have rupture or thickening of the ganglion cell, or have internal bleeding. The sonography is not sufficient in distinguishing such a case from solid tumors in general (Freire *et al.*, 2012).

V. REFERENCES

- Barua, A, Mudunuri, LS & Kosheleva, O 2014, 'Why trapezoidal and triangular membership functions work so well: Towards a theoretical explanation', *Journal of Uncertain Systems*, vol. 8, no.3, pp. 164-168.
- Bruil, E, Efimtcev, AY, Fokin, VA, Fernandez, R, Levchuk, AG, Ogier, AC, Melchakova, IV, Bendahan, D & Andreychenko, A 2018, 'Deep learning-based fully automatic segmentation of wrist cartilage in MR images', *arXiv preprint arXiv:1811.01123*.
- Enikov, ET & Anton, R 2014, 'Image segmentation and analysis of flexion-extension radiographs of cervical spines', *Journal of medical engineering*, vol. 2014 article 976323(online).
- Freire, V, Guérini, H, Campagna, R, Moutounet, L, Dumontier, C, Feydy, A & Drapé, JL 2012, 'Imaging of hand and wrist cysts: a clinical approach', *American Journal of Roentgenology*, vol. 199, no. 5, pp. W618-W628.
- Gonzalez, RC & Woods, RE 2002, *Digital Image Processing*, 2nd edn, Prentice Hall, New Jersey.
- Gress, F, Schmitt, C, Savides, T, Faigel, DO, Catalano, M, Wassef, W, Roubain, L, Nickl, N, Ciaccia, D, Bhutani, M & Hoffman, B 2001, 'Interobserver agreement for EUS in the evaluation and diagnosis of submucosal masses', *Gastrointestinal endoscopy*, vol. 53, no.1, pp.71-76.
- Gude, W & Morelli, V 2008, 'Ganglion cysts of the wrist: pathophysiology, clinical picture, and management', *Current reviews in musculoskeletal medicine*, vol. 1, issue. 3-4, pp.205-211.
- Gupta, R, Elamvazuthi, I, Dass, SC, Faye, I, Vasant, P, George, J & Izza, F 2014, 'Curvelet based automatic segmentation of supraspinatus tendon from ultrasound image: a focused assistive diagnostic method', *Biomedical engineering online*, vol. 13, no. 1, pp.157.
- Head, L, Gencarelli, JR, Allen, M & Boyd, KU 2015, 'Wrist ganglion treatment: systematic review and meta-analysis', *The Journal of hand surgery*, vol. 40, no.3, pp.546-553.
- Kang, SH, Kee, S, Choi, CN, Song, HM & Song, HS 2014, 'Wrist ganglionic cyst with hyperechoic finding in the ultrasonography'. *Journal of Korean Orthopedics Ultrasound Society*, vol. 7, no. 7, pp. 45-48.

IV. CONCLUSIONS

In this paper, we propose an automatic extraction method for finding ganglion cysts in the wrist area from ultrasound images. Ganglion cysts are common muscular skeletal disease that have frequent recurrence rate thus it is important to observe the prognosis even after surgical treatment.

We propose a dynamic fuzzy binarization method with fuzzy stretching for enhancing intensity contrast from the image. In experiment, the proposed method shows clinically meaningful successful extraction rate (93.3% or 42 out of 45 cases) and that was far superior to other binarization methods. We verify that the fuzzy stretching component also contributes to this success as comparing with normalization process.

However, the limitation of this research is that such results are obtained from only wrist area cysts. If we extend this result using more intelligent paradigm (Bruil *et al.*, 2018), it is likely to be helpful in the extraction of ellipsoidal diseases such as lipomas or cystic tumors similar to those of the ganglion other than wrist part as well as similar diseases occurring in various parts of the body.

- Kim, KB & Song, DH 2017, 'Automatic Defect Inspection for Spectacle Lens Products with Fuzzy Stretching', *International Information Institute (Tokyo). Information, 20(1B)*, pp.555-560.
- Kim, KB 2015, 'Extracting Ganglion Cysts from Ultrasound Image with Fuzzy Membership Function', *Journal of the Korea Institute of Information and Communication Engineering*, vol. 19, no. 6, pp. 1296-1300.
- Kim, KB, Song, DH & Lee, WJ 2014, 'Flaw detection in ceramics using sigma fuzzy binarization and gaussian filtering method', *International Journal of Multimedia and Ubiquitous Engineering*, vol. 9, no. 1, pp. 403-414.
- Kim, KB, Song, DH, & Yun, SS 2018, 'Automatic Extraction of Blood Flow Area in Brachial Artery for Suspicious Hypertension Patients from Color Doppler Sonography with Fuzzy C-Means Clustering'. *Journal of information and communication convergence engineering*, vol. 16, no. 4, pp.258-263.
- Kim, KB, Woo, YW & Yang, HK 2006, 'An intelligent system for container image recognition using ART2-based self-organizing supervised learning algorithm', *In Proceedings of Asia-Pacific Conference on Simulated Evolution and Learning*, Springer, Berlin, Heidelberg, pp 897-904
- Kwon, SH, Ryu, KN, Park, YK & Jeong, YM 2001, 'Soft Tissue Masses: Ultrasonographic Findings', *Ultrasonography*, vol. 20, no. 4, pp.349-355.
- Park, J, Song, DH, Han, SS, Joo Lee, S & Kim, KB 2017, 'Automatic extraction of soft tissue tumor from ultrasonography using ART2 based intelligent image analysis', *Current Medical Imaging Reviews*, vol. 13, no. 4, pp.447-453.
- Shin, CH & Jung, CY 2017, 'An Optimal Algorithm for Enhancing the Contrast of Chest Images Using the Frequency Filters Based on Fuzzy Logic', *Journal of Information and Communication Convergence Engineering*, vol. 15, no. 2, pp. 131-136.
- Suen, M, Fung, B & Lung, CP 2013, 'Treatment of ganglion cysts', *ISRN orthopedics*, Volume 2013, Article ID 940615.
- Suryadibrata, A & Kim, KB 2017, 'Ganglion Cyst Region Extraction from Ultrasound Images Using Possibilistic C-Means Clustering Method', *Journal of information and communication convergence engineering*, vol. 15, no. 1, pp.49-52.
- Suryadibrata, A, Song, DH & Kim, KB 2017, 'Automatic Ganglion Cyst Detection from Ultrasound Images using Fuzzy C-Means Clustering Method', *International Information Institute (Tokyo). Information, 20(4A)*, pp.2543-2548.
- Wang, G, Jacobson, JA, Feng, FY, Girish, G, Caoili, EM & Brandon, C 2007, 'Sonography of wrist ganglion cysts: variable and noncystic appearances', *Journal of ultrasound in medicine*, vol. 26, no. 10, pp.1323-1328.
- Woo, HS & Kim, KB 2016, 'Improved Fuzzy Binarization Method with Trapezoid type Membership Function and Adaptive α _cut', *Journal of the Korea Institute of Information and Communication Engineering*, vol. 20, no. 10, pp. 1852-1859.
- Yamazaki, H, Kato, H & Murakami, N 2007, 'Closed rupture of the flexor tendons of the index finger caused by a pathological fracture secondary to an intraosseous ganglion in the lunate', *Journal of Hand Surgery (European Volume)*, vol. 32, no. 1, pp.105-107.
- Yoo, HJ 2014, 'Sonographic Features of Common Soft Tissue Masses in the Extremities', *Journal of the Korean Orthopaedic Association*, vol. 49, no. 6, pp.422-430.